The pseudophosphatase MK-STYX interacts with G3BP and decreases stress granule formation

Shantá D. HINTON*†, Michael P. MYERS*[1], Vincent R. ROGGERO‡, Lizabeth A. ALLISON‡ and Nicholas K. TONKS*[2]

*Cold Spring Harbor Laboratory, 1 Bungtown Road, Cold Spring Harbor, NY 11724, U.S.A., †Department of Biological Sciences, 101 Dupont Hall, Hampton University, Hampton, VA 23668, U.S.A., and ‡Department of Biology, 3030 Integrated Science Center, College of William and Mary, Williamsburg, VA 23187, U.S.A.

MK-STYX [MAPK (mitogen-activated protein kinase) phospho-serine/threonine/tyrosine-binding protein] is a pseudo-phosphatase member of the dual-specificity phosphatase subfamily of the PTPs (protein tyrosine phosphatases). MK-STYX is catalytically inactive due to the absence of two amino acids from the signature motif that are essential for phosphatase activity. The nucleophilic cysteine residue and the adjacent histidine residue, which are conserved in all active dual-specificity phosphatases, are replaced by serine and phenylalanine residues respectively in MK-STYX. Mutations to introduce histidine and cysteine residues into the active site of MK-STYX generated an active phosphatase. Using MS, we identified G3BP1 [Ras-GAP (GTPase-activating protein) SH3 (Src homology 3) domain-binding protein-1], a regulator of Ras signalling, as a binding partner of MK-STYX. We observed that G3BP1 bound to native MK-STYX; however, binding to the mutant catalytically active form of MK-STYX was dramatically reduced. G3BP1 is also an RNA-binding protein with endoribonuclease activity that is recruited to 'stress granules' after stress stimuli. Stress granules are large subcellular structures that serve as sites of mRNA sorting, in which untranslated mRNAs accumulate. We have shown that expression of MK-STYX inhibited stress granule formation induced either by aresenite or expression of G3BP itself; however, the catalytically active mutant MK-STYX was impaired in its ability to inhibit G3BP-induced stress granule assembly. These results reveal a novel facet of the function of a member of the PTP family, illustrating a role for MK-STYX in regulating the ability of G3BP1 to integrate changes in growth-factor stimulation and environmental stress with the regulation of protein synthesis.

Key words: dual-specificity phosphatase, mitogen-activated protein kinase serine-, threonine- and tyrosine-specific phosphatase (MK-STYX), pseudophosphatase, Ras-GTPase-activating protein Src-homology-3-domain-binding protein-1 (G3BP1), stress granule.

INTRODUCTION

A crucial aspect of signal transduction is the organization of networks of protein–protein interactions, which is facilitated by reversible protein phosphorylation, mediated by protein kinases and phosphatases. Whereas the kinases have been implicated in controlling the amplitude of a signalling response, phosphatases are thought to play a greater role in controlling the rate and duration of the response [1,2]. Thus the co-ordinated and competing activities of kinases and phosphatases are important for determining signalling outcome. Furthermore, disruption of the normal patterns of protein phosphorylation results in aberrant regulation of signal transduction and this has been implicated in the aetiology of a variety of major human diseases, including cancer, diabetes, inflammation and neurodegeneration.

Unlike the protein kinases, which are derived from a common ancestor, the protein phosphatases have evolved in separate families that are structurally and mechanistically distinct. PTPs (protein tyrosine phosphatases), which are defined by the active-site signature motif $HC(X)_5R$, are divided into the classical pTyr (phosphotyrosine)-specific phosphatases and the DSPs (dual-specificity phosphatases) [3]. In general, they share the same catalytic mechanism, but the conformation of the DSP active site allows them to accommodate pSer (phosphoserine)/pThr (phosphothreonine) residues, as well as pTyr residues in proteins. Nonetheless, in terms of physiological function, the 'DSPs' may actually show preference for either pTyr or pSer/pThr residues *in vivo*. Some even target non-protein substrates, such as inositol phospholipids and RNA. It is now apparent that the PTPs do not simply function as passive antagonists of the PTKs (protein tyrosine kinases), but rather are critical regulators of signalling in their own right and have the capacity to act both positively and negatively in the control of signal transduction. Furthermore, the PTPs display exquisite substrate, and functional, specificity *in vivo*. More recently, it has become apparent that within this family there are several pesudophosphatases, which are members that possess conserved domains with core features of a PTP, but which lack residues that are essential for catalysis [3–5]. A similar situation exists within the protein kinase family, such as in the example of STRAD (Ste20-related adaptor), which is a Ste20-like pseudokinase that regulates the function of the tumour suppressor kinase LKB1 [6].

The prototypic pseudophosphatase STYX (phosphoserine/ threonine/tyrosine-binding protein) is catalytically inactive

because it features a glycine residue at the position expected for the active-site cysteine residue [7]. In fact, a single-point mutation that converts the glycine residue into cysteine was sufficient to generate a mutant protein with activity similar to a *bona fide* DSP [7]. It was proposed initially that STYX represented a new class of pSer/pThr/pTyr-binding proteins, a naturally occurring example of a substrate-trapping mutant [8,9] that functions as an antagonist of endogenous protein phosphatases. Disruption of the *STYX* gene in mice revealed an essential function in spermatogenesis; the knockout mice were defective for sperm production [10]. STYX co-immunoprecipitates with a spermatid phosphoprotein, CRHSP-24 (calcium-responsive heat-stable protein with a molecular mass of 24 kDa), which is a unique RNA-binding protein [10]. However, the molecular details of the function of this catalytically impaired pseudophosphatase and the importance of the association with CRHSP-24 remain to be defined.

Further examples of pseudophosphatases within the PTP family include certain RPTPs (receptor PTPs). IA2 (islet cell antigen 512) (PTPRN) is a major auto-antigen in Type 1 diabetes [11]. It contains a single PTP domain that adopts the structure of a classical PTP fold [12,13]; however, there are substitutions of at least three catalytically essential residues in the PTP domain of IA2. Back-mutation of these residues to the consensus found in an active PTP domain was sufficient to restore activity [14]. The mechanism of action of IA2 remains unclear, but several interacting proteins have been identified [15]. Unlike IA2, most RPTPs contain a tandemly repeated arrangement of intracellular PTP domains, in which the membrane-proximal D1 domain is catalytically active, whereas it is the membrane-distal D2 domain that maintains a PTP fold, but lacks critical residues for activity. In LAR, only two point mutations are required to convert its D2 domain into an active PTP [16]. This situation is again reminiscent of examples encountered among the protein kinases. Like the RPTPs, the PTK JAK (Janus kinase) contains both an active and a pseudokinase domain; the latter suppresses the activity of the catalytic domain and is mutated in the myeloproliferative disease polycythaemia vera, leading to enhanced JAK activity [17]. The function of RPTP D2 domains remains unclear, although a potential role as redox sensors has been proposed [18].

There are also further examples of pseudophosphatases within the DSPs. In *Caenorhabditis elegans*, the pseudophosphatases EGG-4 and EGG-5 bind to, and regulate signalling by, the DYRK (dual-specificity tyrosine-phosphorylated and -regulated kinase) family kinase MBK2 (mini brain kinase 2) [5,19]. The pseudophosphatases are most prevalent among the MTMs (myotubularins) [20]. Of the 14 MTM genes in the human genome, six encode pseudophosphatases [21]. It has been shown that inactive MTMs may serve a scaffolding function, forming complexes with the active enzymes, to regulate both catalytic function and the subcellular location of the active phosphatase. For example, the active enzyme MTMR2 (MTM-related protein 2) binds the pseudophosphatase MTMR13 [22]. Inactivating mutations in MTMR2 have been associated with type 4B CMT (Charcot–Marie–Tooth) disease, a neuropathy characterized by abnormal nerve myelination [20]. It is interesting to note that mutations in the pseudophosphatase MTMR13 also give rise to type 4B CMT disease [22,23], which is consistent with the significance of the interaction between MTMR2 and MTMR13 and the functional importance of the pseudophosphatase component.

In the present study, we have focused on a different pseudophosphatase, called MK-STYX [MAPK (mitogen-activated protein kinase)-STYX] [DUSP24 (dual-specificity phosphatase)], of which little is known except that it is highly expressed in Ewing's sarcoma family tumours [24]. MK-STYX

is structurally related to the DSPs, in particular the MAPK phosphatases, which dephosphorylate both the threonine and tyrosine residues in the activation loop of members of the MAPK family [3,25]. MK-STYX lacks the essential catalytic cysteine and adjacent histidine residues from the PTP signature motif. We have demonstrated that introduction of point mutations at the 'active site' of MK-STYX to generate a consensus signature motif is sufficient to generate an active enzyme. Unexpectedly, we observed that MK-STYX formed a complex with G3BP [Ras-GAP (GTPase-activating protein) SH3 (Src homology 3)-domain-binding protein]. Formation of this complex was impaired with the catalytically active mutant form of MK-STYX. G3BP is a phosphorylation-dependent endoribonuclease that is an effector of stress granule formation [26]. We have demonstrated that expression of MK-STYX significantly inhibited formation of stress granules, which is consistent with a role as a regulator of mRNA stability in stress-response pathways.

EXPERIMENTAL

Plasmid constructs

The N-terminal and C-terminal ends of human MK-STYX (GenBank® accession number NM_016086.2) were flanked with a FLAG epitope tag, and PstI and EcoRI restriction sites by PCR. The PCR product was ligated into PstI and EcoRI sites of the mammalian expression vector pMT2 to create pMT2-FLAG-MK-STYX-FLAG. The QuikChange™ Site-Directed Mutagenesis Kit (Stratagene) was used to make the substitutions F245H and S246C to construct the active mutant form of MK-STYX, designated MK-STYX$_{active}$, in the expression vector pMT2-FLAG-MK-STYX$_{active}$-FLAG. The integrity of all constructs derived from PCR was confirmed by DNA sequencing. The G3BP–GFP (green fluorescent protein) construct was kindly provided by Dr Jamai Tazi (Institut de Génétique Moléculaire, Montpellier, France).

Cell culture and transient transfection

COS-1 cells and HEK-293 (human embryonic kidney) cells were maintained at 37°C, 5% CO_2, in DMEM (Dulbecco's modified Eagle's medium) supplemented with 10% FBS (fetal bovine serum) and 1% penicillin/streptomycin (Invitrogen). HeLa cells were maintained under similar conditions, except they were cultured in MEM (minimal essential medium) (Invitrogen) supplemented with 10% FBS. Transfections were performed using FuGENE™ 6 reagent (Roche Applied Science), Lipofectamine™ or Lipofectamine™ 2000 reagent (Invitrogen).

Assay of protein phosphatase activity

COS-1 cells were transfected either with expression vector for native MK-STYX (pMT2-FLAG-MK-STYX-FLAG) or the catalytically active mutant MK-STYX (pMT2-FLAG-MK-STYX$_{active}$-FLAG). Post-transfection (48 h), cells were lysed and MK-STYX proteins were immunoprecipitated using anti-FLAG antibodies (Sigma). Phosphatase activity in the immunoprecipitates was assayed by incubation with ^{32}P-labelled poly(Glu-Tyr) as the substrate (5 mM pTyr-protein) at 30°C in 25 mM imidazole (pH 7.2), 0.1 mg/ml BSA and 1 mM DTT (dithiothreitol). Poly(Glu-Tyr) (4:1) (Sigma) was phosphorylated with b-IRK (baculovirus insulin receptor kinase) in the presence of [γ-^{32}P]ATP [27].

Metabolic labelling and MS

Post-transfection (48 h), COS-1 cells were incubated for 30 min in DMEM minus methionine (Invitrogen), supplemented with

10% dialysed FBS and 1:100 L-glutamine. Subsequently, cells were incubated for 3 h in medium containing 0.15 mCi of [35S]-labelled methionine, and tagged MK-STYX proteins were immunoprecipitated from cell lysates with anti-FLAG antibodies (Sigma). Samples were analysed by SDS/PAGE (10% gels) and autoradiography, or by MS. For MS, immunoprecipitates were incubated with EZview™ Red ANTI-FLAG® M2 Affinity Gel (Sigma). The samples were trypsinized from EZview™ Red ANTI-FLAG® M2 Affinity Gel (Sigma), and analysed by LC-MS/MS (liquid chromatography–tandem MS).

Immunoprecipitation and immunoblotting

Post-transfection (48 h), HEK-293 cells were harvested in lysis buffer [50 mM Hepes, pH 7.2, 150 mM NaCl, 1 mM sodium vanadate, 10% glycerol, 10 mM NaF, 1% Nonidet P-40 Alternative (Calbiochem), 1 mM PMSF, 1 mM benzamidine, 5 mg/ml aprotinin and 5 mg/ml leupeptin]. Lysates were centrifuged at 14000 g for 10 min, and the supernatant protein concentration was determined with the Bradford reagent. Lysates were resolved by SDS/PAGE (10% gels) and transferred on to a PVDF membrane (GE Healthcare) for immunoblot analysis with anti-FLAG (Sigma) and anti-G3BP (BD Bioscience) antibodies, followed by chemiluminescent detection. X-ray films were quantified by scanning densitometry using ImageJ software (National Institutes of Health). For immunoprecipitation, the lysates were pre-cleared, then incubated with anti-FLAG or anti-G3BP antibody for 1 h at 4°C. Samples were washed three times in lysis buffer and boiled in Laemmli sample buffer. To determine G3BP expression levels by immunoblotting, HeLa cell lysates were prepared 24 h post-transfection and replicate blots were probed with anti-FLAG, anti-G3BP or anti-β-tubulin (1:200 dilution) (Santa Cruz Biotechnology) antibodies.

Transient transfection and cell imaging

For immunofluorescence, HeLa cells were grown to 80–90% confluence and 2×10^5 cells were plated on to coverslips in six-well dishes (Nunc). Post-plating (24 h), cells at 40–60% confluence were transfected with 2 mg of G3BP–GFP, pMT2, or wild-type or mutant FLAG-tagged MK-STYX expression plasmid DNA and 4 ml of Lipofectamine™ 2000 reagent per well, according to the manufacturer's protocol. The medium was replaced with fresh medium at least 4 h before fixation and staining. Post-transfection (24 h), cells were washed with PBS, fixed with 3.7% formaldehyde and permeabilized with 0.2% Triton X-100. The coverslips were mounted on to a slide using GelMount containing DAPI (4′,6-diamidino-2-phenylindole; 0.5 mg/ml; Sigma). Expression of FLAG-tagged MK-STYX was confirmed by immunofluorescence.

For experiments examining the effect of MK-STYX on stress-induced stress granule formation, at 23 h post-transfection, HeLa cells were treated with 500 μM sodium arsenite (Sigma) for 1 h, then processed as above. To visualize stress granule formation, endogenous G3BP was used as the marker and visualized with anti-G3BP (1:100 dilution) and Cy3 (indocarbocyanine)-conjugated goat anti-mouse (1:200; Zymed Laboratories) antibodies.

Counting and image collection were performed on either of two microscopes. For some analyses, an inverted Nikon ECLIPSE TE 2000-E fluorescence microscope, with a Nikon Ultraviolet Excitation UV-2E/C filter block for DAPI visualization, and a Blue Excitation B-2E/C filter block for G3BP–GFP visualization, were used with a Nikon Plan Apo 40 × /0.95 NA (numerical aperture) objective. A CoolSNAP HQ$_2$ CCD (charge-coupled-device) camera (Photometrics) and NIS-Elements AR software (Nikon) were used for image acquisition and primary image processing. For other analyses, an Olympus BX60 microscope with U-MNU filter cube for DAPI and Omega Optical XF100-2 for GFP were used with an Olympus 40XUPlanFL 40 × /0.75 NA objective. A Cooke SensiCam^{QE} camera and IPlab software (BD Biosciences Bioimaging) were used for image acquisition and primary image processing. ImageJ and Adobe Photoshop CS3/IllustratorCS3 were also used for any secondary image processing.

Approx. 400 cells were scored per treatment. Samples were scored blind with regard to treatment and were scored independently by two different individuals. Cells were scored in three categories: no stress granules, intermediate stress granules or complete stress granules. Intermediate stress granules were characterized as smaller granules dispersed throughout the cytoplasm. Complete stress granules were characterized as large granule aggregates that formed around the nucleus.

RESULTS

Pseudophosphatase MK-STYX can be converted into a catalytically active phosphatase

Database analysis was used to construct and clone a full-length cDNA encoding the protein MK-STYX, which is the product of the *DUSP24* gene. Full-length MK-STYX displays homology with the MKPs (MAPK phosphatases), such as MKP1 [3,25]. The consensus active-site signature motif for members of the PTP family is [I/V]**H**CXXG**XX**R[S/T], in which the residues in bold play critical roles in catalysis. In the catalytically functional DSP MKP1, this motif is V**H**CQAGIS**R**S, whereas in MK-STYX the equivalent sequence is I**F**STQGIS**R**S. In the light of the absence of the adjacent histidine and cysteine residues in the signature motif, it would be anticipated that wild-type MK-STYX would have limited catalytic competence. This was confirmed in assays of activity in immunoprecipitates of MK-STYX from transiently transfected COS-1 cells overexpressing the protein (Figure 1). To test whether a catalytically competent form of MK-STYX could be generated, we altered its signature motif by site-directed mutagenesis to convert Phe-245 and Ser-246 into the histidine and cysteine residues respectively, which are characteristic of the signature motif of an active PTP family member. These changes were sufficient to generate a catalytically functional mutant form of MK-STYX that recognized [32P]-labelled poly(Glu-Tyr) as a substrate (Figure 1).

Identification of MK-STYX-binding proteins

Of the pseudophosphatase members of the PTP family studied to date, a consistent theme is the functional importance of protein–protein interactions. In order to gain insights into the function of MK-STYX, we initiated a search for potential binding partners. We transfected COS-1 cells with expression vectors for either FLAG-tagged MK-STYX or the MK-STYX$_{active}$ mutant protein, metabolically labelled the cells with [35S]-methionine, and immunoprecipitated the proteins with anti-FLAG antibodies. Although there was some overlap in the binding pattern, it was interesting to note that some proteins interacted specifically with the wild-type catalytically suppressed form of MK-STYX, but not the catalytically competent mutant form of the protein (Figure 2). These differences in binding highlight the potential functional importance of wild-type MK-STYX-specific interacting proteins.

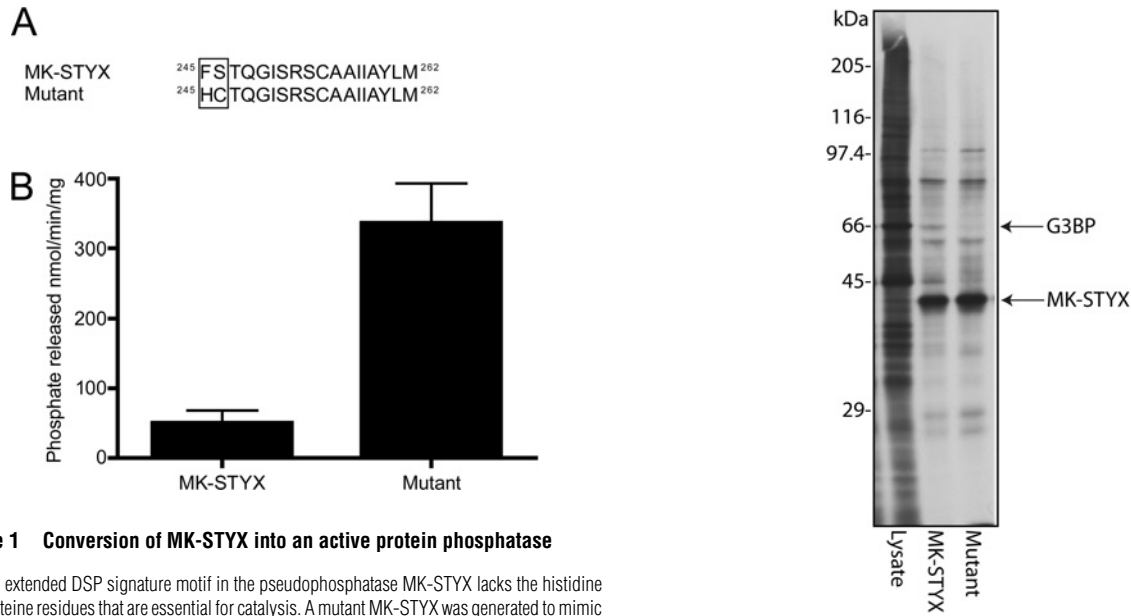We analysed the MK-STYX-containing protein complexes by MS. Our analysis confirmed the presence of MK-STYX and

Figure 1 Conversion of MK-STYX into an active protein phosphatase

(**A**) The extended DSP signature motif in the pseudophosphatase MK-STYX lacks the histidine and cysteine residues that are essential for catalysis. A mutant MK-STYX was generated to mimic a functional DSP by substituting histidine in place of phenylalanine at residue 245 and cysteine in place of serine at residue 246. (**B**) Wild-type and mutant MK-STYX were expressed in COS cells, immunoprecipitated and assayed for phosphatase activity against poly(Glu-Tyr) (4:1) as substrate. Three replicate experiments were performed. The results are the means ± S.E.M.

MK-STYX$_{active}$ in the appropriate samples, and identified a number of proteins as possible binding partners. In the light of the structural features of MK-STYX, and considering the precedent of the MTMs [21], we predicted that it might form a complex with an active phosphatase. However, we did not detect such an interaction. Unexpectedly, the major binding partner of wild-type MK-STYX that we identified by MS was not a phosphatase, but an RNA-binding protein, G3BP, which resolves as a 68 kDa protein by SDS/PAGE [28]. In contrast, G3BP was not a significant component of the complex that co-immunoprecipitated with MK-STYX$_{active}$.

Figure 2 Identification of MK-STYX-binding partners

COS-1 cells were transfected with expression vectors for FLAG-tagged wild-type and active mutant MK-STYX, metabolically labelled with [^{35}S]methionine, and immunoprecipitated with anti-FLAG antibodies. Binding proteins were resolved by SDS/PAGE and visualized by autoradiography. Molecular masses are indicated on the left-hand side.

Interaction of MK-STYX with G3BP

To confirm that G3BP was a binding partner of MK-STYX, we co-transfected HEK-293 cells with expression vectors for GFP-tagged G3BP and either FLAG-tagged MK-STYX or MK-STYX$_{active}$ mutant. We immunoprecipitated MK-STYX with anti-FLAG antibodies, and observed, by immunoblotting, that more wild-type MK-STYX co-precipitated with G3BP than the MK-STYX$_{active}$ mutant when they were expressed at similar levels (Figure 3A). This confirms the observation in our MS analysis
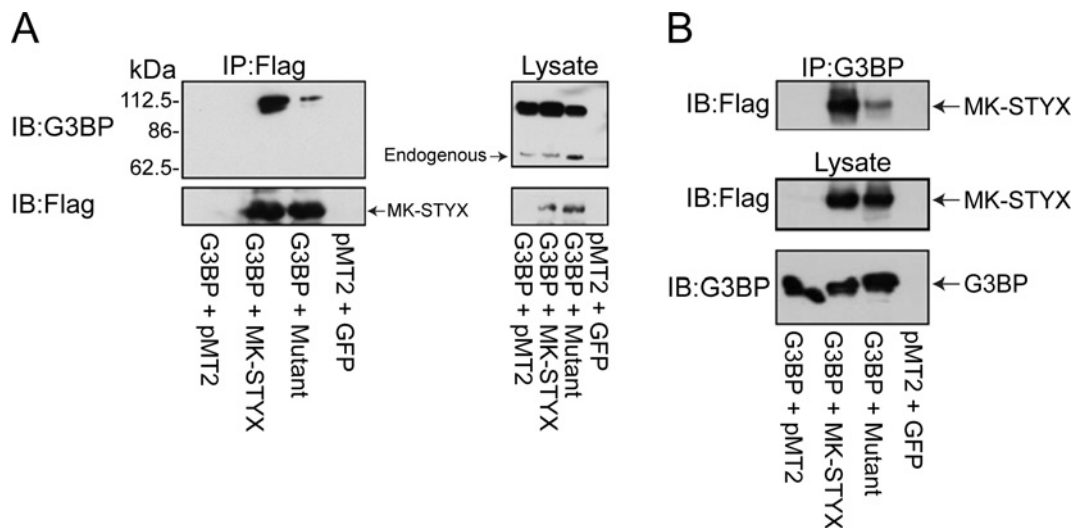

Figure 3 Interaction of G3BP1 and MK-STYX

HEK-293 cells were co-transfected with expression vectors for FLAG-tagged MK-STYX, mutant active MK-STYX or empty vector pMT2, and G3BP–GFP or vector pEGFP. (**A**) MK-STYX was immunoprecipitated (IP) from cell lysates with anti-FLAG antibodies, and (**B**) G3BP1 was immunoprecipitated from cell lysates with anti-G3BP antibodies, in each case followed by immunoblotting (IB) with anti-FLAG and anti-G3BP antibodies to investigate the extent of binding. Similar results were obtained from multiple replicate experiments.
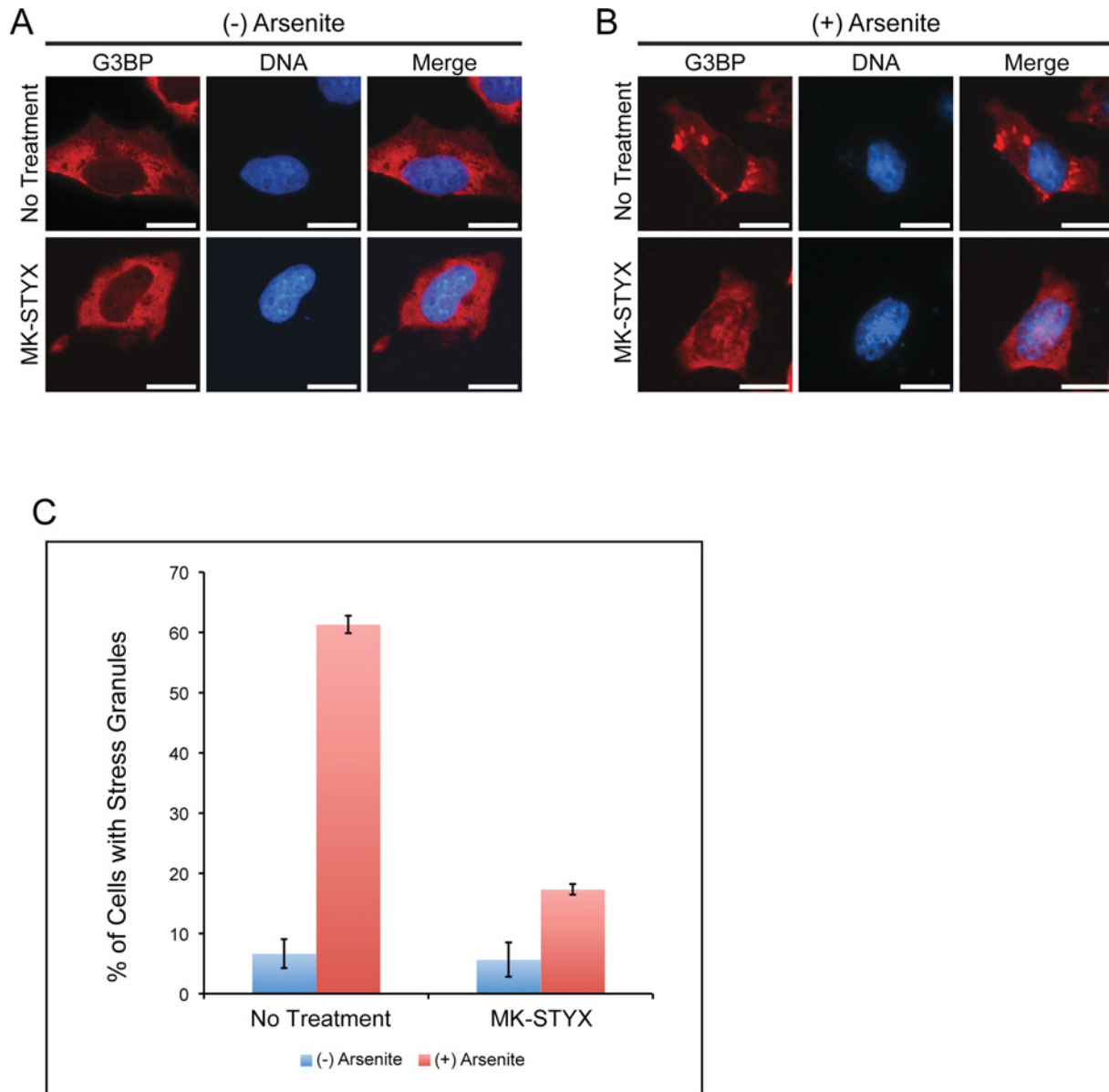
Figure 4   Inhibition of arsenite-induced stress granule formation by MK-STYX

Representative examples are presented to illustrate the subcellular distribution of endogenous G3BP1 without arsenite treatment (**A**) or following stimulation with 500 μM sodium arsenite (**B**) in the absence (No Treatment) or presence of MK-STYX. Cells were fixed, stained with anti-G3BP and Cy3-conjugated goat anti-mouse antibodies and DAPI, and analysed 24 h post-transfection for arsenite-induced stress granule formation by fluorescence microscopy. Merged images show the location of endogenous G3BP (red) relative to the DAPI-stained nucleus (blue). Scale bar, 10 μm. (**C**) Cells were scored for the presence and absence of stress granules. Three replicate experiments were performed ($n = 100$ cells for each experiment); the results are the means $\pm$ S.E.M.

(Figure 2). The preference for interaction between G3BP and wild-type MK-STYX, rather than MK-STYX$_{active}$ mutant, was also observed in the reciprocal experiment in which we immunoprecipitated with anti-G3BP antibodies (Figure 3B) and immunoblotted for the presence of MK-STYX. Taken together, these experiments confirm that MK-STYX and G3BP were binding partners in a cellular context and, furthermore, that the interaction was disrupted by mutation to convert MK-STYX into an active phosphatase.

Expression of MK-STYX decreased stress granule formation

The assembly of stress granules is triggered following stimulation of cells with arsenite [29]. This process can be visualized by the change in intracellular localization of endogenous G3BP,

from a diffuse distribution throughout the cytoplasm to the large stress granule structures. In order to test whether MK-STYX could affect this process, we compared the effects of arsenite on localization of endogenous G3BP in HeLa cells transfected before and after ectopic expression of MK-STYX. These cells were chosen both to avoid any cell line bias in our present study of the interaction and because they had been used previously in the study of G3BP [32]. The expression of endogenous G3BP1 was visualized by staining with anti-G3BP1 and Cy3-conjugated secondary antibody and analysed by fluorescence microscopy (Figure 4). Exposure to arsenite induced stress granule formation in approx. 60 % of non-transfected cells, whereas expression of MK-STYX resulted in a dramatic decrease in stress granule formation; only approx. 18 % of HeLa cells transfected with

the MK-STYX expression plasmid formed stress granules (Figure 4).

Stress granule formation has also been shown to be induced by overexpression of G3BP alone [29]. Therefore we tested whether expression of MK-STYX affected stress granule induction by G3BP. To this end, we co-transfected GFP-tagged G3BP with FLAG-tagged MK-STYX or MK-STYX$_{active}$ mutant in HeLa cells. The expression of G3BP–GFP was analysed by fluorescence microscopy and cells were scored for stress granule formation (Figure 5). Three categories were established: no stress granules, complete stress granules (granules are large and perinuclear) and intermediate stress granules (smaller aggregates dispersed throughout the cytoplasm) (Figure 5A). Overexpression of G3BP in HeLa cells induced stress granules in approx. 50 % of transfected cells (Figure 5B). Strikingly, in cells co-transfected with the G3BP and MK-STYX expression plasmids only approx. 20 % of transfected cells formed stress granules, suggesting that expression of MK-STYX inhibited stress granule assembly. One possible explanation for this reduced stress granule formation is that expression of MK-STYX somehow suppressed expression of G3BP. However, there was no significant difference in the expression levels of G3BP when transfected alone or together with either the empty vector or the expression vector for MK-STYX (Figure 5C). There was an intermediate effect of expression of MK-STYX$_{active}$ mutant, in which approx. 37 % of cells co-transfected with G3BP and MK-STYX$_{active}$ displayed stress granules (Figure 5B). Thus the production of an enzymatically active form of MK-STYX not only impaired the interaction with G3BP, but also attenuated its inhibitory effect on stress granule formation. Interestingly, cells expressing the MK-STYX$_{active}$ mutant displayed more intermediate stress granules (smaller aggregates) compared with those expressing G3BP alone (Figure 5A), suggesting that the catalytically active form of MK-STYX slowed the process of stress granule formation, but did not completely repress assembly.

DISCUSSION

Several pseudophosphases have been identified within the PTP family. Their sequences suggest that they will adopt a PTP fold, but residues that are essential for catalysis are missing and therefore these members of the PTP family will lack intrinsic phosphatase activity [3,5]. Investigations into the mechanism by which these pseudophosphatases affect signalling pathways have highlighted the importance of protein–protein interactions. In the present paper, we report a novel interaction between the pseudophosphatase MK-STYX and G3BP, a regulator of Ras function and stress granule assembly. G3BP is an RNA-binding protein, presenting an interesting symmetry between MK-STYX and the prototypic pseudophosphatase STYX, which interacts with the spermatid RNA-binding protein CRHSP-24 [10]. We have demonstrated that the introduction of two point mutations in the signature motif of MK-STYX was sufficient to convert it into an active phosphatase. Interestingly, G3BP bound preferentially to the native phosphatase-dead form of MK-STYX. Furthermore, this interaction significantly reduced the formation of stress granules induced either by arsenite treatment or by expression of G3BP.

G3BP1 is a member of a small family of three ubiquitously expressed proteins, derived from two distinct genes in humans. The second member, G3BP2, exists in two differentially spliced forms [26]. The N-terminus of the G3BPs is characterized by the presence of a NTF (nuclear transport factor) 2-like domain and a segment rich in acidic residues. The central segment contains proline-rich PXXP motifs, and the C-terminal portion of the proteins is characterized by motifs associated with RNA binding, including a canonical RNA recognition motif and an arginine- and glycine-rich RGG box. G3BP1 is defined as a Ras-GAP SH3-domain-binding protein, due to a Ras-GTP-dependent interaction between the NTF2 domain of G3BP1 and the SH3 domain of GAP in proliferating cells. Interestingly, the G3BP homologue in *Drosophila*, *rasputin* (*rin*), interacts genetically with the Ras signalling pathway [30]. G3BP1 is highly phosphorylated on multiple serine residues in quiescent cells, but changes in the pattern of phosphorylated residues accompany proliferation [31]. In particular, the absence of a phosphate group on Ser-149 in proliferating cells was shown to be dependent on Ras-GAP and also to influence the subcellular distribution of G3BP1 [31,32]. However, stimulation of breast cancer cells with the EGF (epidermal growth factor) receptor ligand Heregulin has also been shown both to induce expression and to enhance phosphorylation of G3BP1 [33], hence the functional importance of G3BP1 phosphorylation will require further clarification. Expression of G3BP1 was also shown to be increased in various tumours and to be associated with enhanced proliferation [34], but the precise role of G3BP1 in the regulation of Ras signalling and the control of proliferation remains unclear.

G3BPs were originally identified as displaying features of RNA-binding proteins and are found in various messenger ribonucleoprotein particles that regulate mRNA processing, transport, translation and decay [26]. In particular, G3BP1 has been identified as a component of stress granules [29]. When cells are exposed to environmental stresses, such as heat shock, UV irradiation, hypoxia or oxidative stress, they initiate protective responses to enhance their survival. One of the most rapid of these is a reversible regulation of mRNA translation to promote expression of proteins that allow the cell to adapt to the stress [35,36]. Formation of stress granules is triggered by phosphorylation of eIF2a (eukaryotic translation initiation factor 2a) under the action of several stress-activated kinases [37], which reduces the initiation of translation. In recent years, there has been a rapid expansion in our understanding of the role of stress granules and G3BP in this response to cellular stress. Stress granules are cytoplasmic storage sites for abortive translation initiation complexes, which act as sorting stations from which mRNAs can be routed to other sites of storage, re-initiation of translation or degradation. They represent a complex assembly of translation initiation factors, such as eIF3 and eIF4E, proteins involved in translational control, such as TIA-1 (T-cell intracellular antigen 1), and proteins implicated in RNA remodelling or degradation, including G3BP1 [35]. Endoribonucleases catalyse mRNA degradation, particularly those mRNAs for which turnover rates are regulated by extracellular stimuli [35,36]. A unique feature of G3BP1 is that it possesses endoribonuclease activity that is regulated by site-specific phosphorylation [32]. The association with Ras-GAP regulates the phosphorylation status, particularly of Ser-149, and the subcellular location of G3BP1, which is consistent with a role for G3BP1 as a sensor that can integrate changes in growth-factor stimulation and environmental stress with the regulation of protein synthesis.

Not only is G3BP1 recruited to stress granules in response to cellular stresses, such as arsenite, but also stress granule assembly can be induced by G3BP1 overexpression alone in transiently transfected cells [29]. Dephosphorylation of G3BP1 at Ser-149 is important in this process, as it enhances its endoribonuclease activity, induces self aggregation and promotes stress granule assembly. Our results have revealed a new component of this cellular response mechanism. We have demonstrated that the interaction of the pseudophosphatase MK-STYX with G3BP
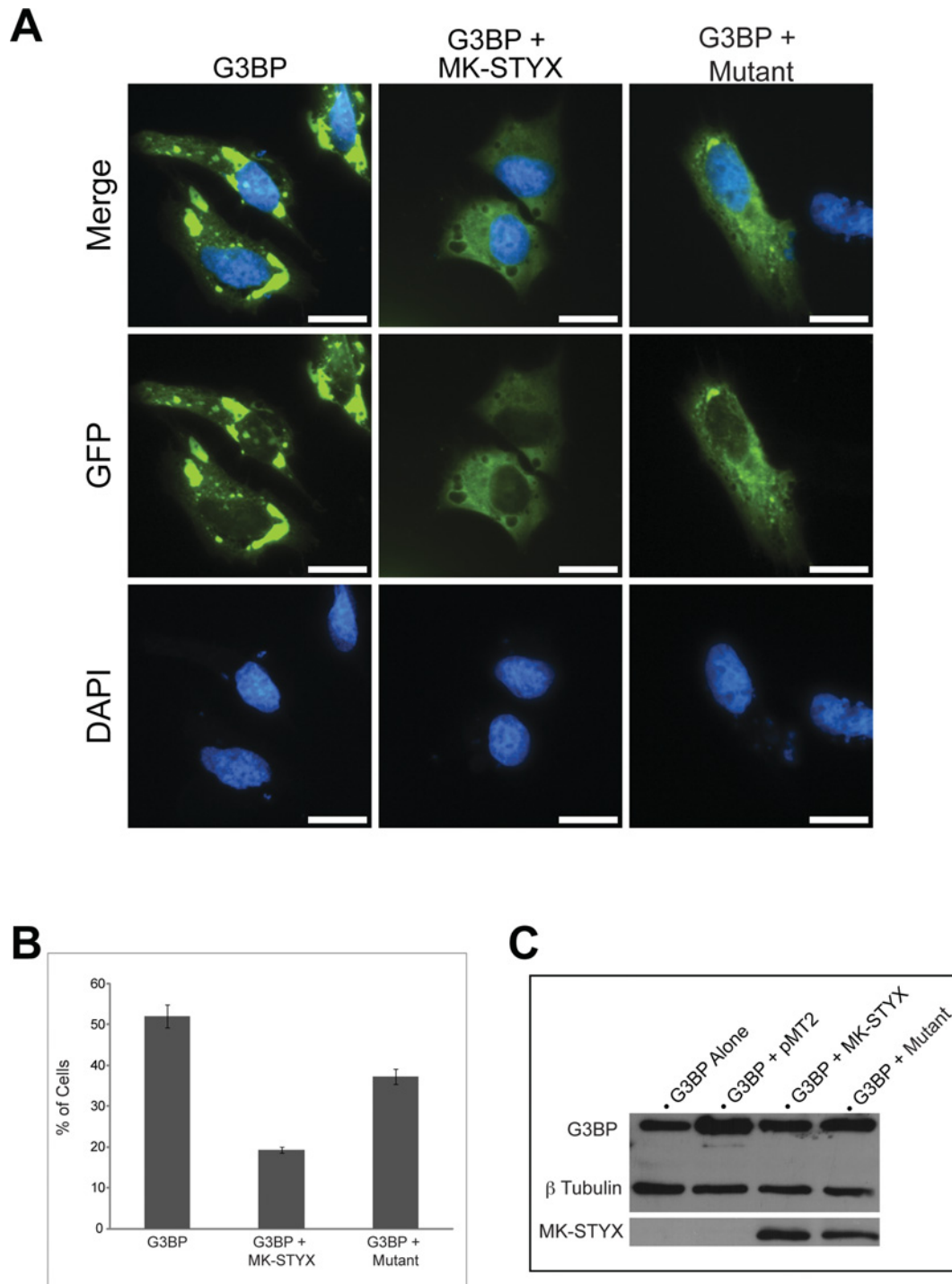
Figure 5   Inhibition of G3BP1-induced stress granule formation by MK-STYX

(**A**) Representative examples of the subcellular distribution patterns of G3BP1. HeLa cells co-transfected with expression vectors for G3BP and either wild-type or active mutant MK-STYX showed fewer cells with fully formed stress granules. The overexpression of G3BP1 alone resulted in mostly complete perinuclear stress granule formation. Cells co-transfected with G3BP1 and the active MK-STYX mutant accumulated smaller granules that were more dispersed throughout the cytoplasm, which may represent intermediates in stress granule formation. Merged images show the location of GFP-tagged G3BP1 (green) relative to the DAPI-stained nucleus (blue). Scale bar, 10 μm. (**B**) HeLa cells were co-transfected with expression vectors for G3BP1–GFP and either MK-STYX or MK-STYX$_{active}$ mutant. Cells were analysed 24 h post-transfection for G3BP-induced stress granule formation by fluorescence microscopy, after staining with the DNA stain DAPI to reveal the nucleus. Cells were scored for the presence or absence of stress granules. Three replicate experiments were performed ($n = 400$); the results are the means $\pm$ S.E.M. (**C**) HeLa cells were transfected with G3BP1–GFP expression vector alone, or co-transfected with G3BP1–GFP expression vector and empty vector (pMT2), or expression vectors for wild-type or active mutant MK-STYX. Post-transfection (24 h), cells were lysed and immunoblotted. Replicate blots were probed with anti-FLAG antibody alone, to visualize MK-STYX, or probed simultaneously with both anti-G3BP and anti-β-tubulin antibodies. Representative immunoblots are shown.

inhibited stress granule formation, whereas expression of the catalytically active mutant MK-STYX led to an accumulation of smaller intermediate-sized aggregates. The fact that MK-STYX is a member of the PTP family of regulators of signal transduction illustrates another potential link between extracellular signals and stress granule assembly. However, the precise mechanism underlying the effects of MK-STYX remains to be defined. It is interesting to note that the catalytically active mutant form of MK-STYX neither bound to G3BP1 nor impaired stress granule formation induced by expression of G3BP to the same extent as native inactive MK-STYX, highlighting the importance of the protein–protein interaction. It has been shown that G3BP1 is phosphorylated on multiple sites in a cellular context [31,32]. In the light of the fact that MK-STYX is a pseudophosphatase, and thus one aspect of its participation in protein–protein interactions may involve the recognition of phosphorylated amino acids in the target protein, it will be interesting to determine the importance of Ser-149 and the other phosphorylation sites in G3BP1 in this interaction.

Changes in expression of both MK-STYX and G3BP1 have been linked to tumorigenesis. In Ewing's sarcoma, a specific chromosomal translocation that fuses the human ETS oncogene FLI1 (Friend leukaemia virus integration 1) to the *EWS* gene leads to expression of the EWS-FLI1 transcription factor, resulting in overexpression of MK-STYX [24]. G3BP levels are regulated by PTEN (phosphatase and tensin homologue deleted on chromosome 10) [38] and HER2 [33]. Furthermore, expression of G3BP1 has been implicated in the regulation of p53 [39]. It has been reported that formation of stress granules inhibits apoptosis in response to cellular stress by suppressing the activation of p38 and JNK MAPKs [40]. Thus further characterization of the functional interplay between MK-STYX and G3BP1 may generate new insights into tumorigenesis and potential approaches to therapy.

AUTHOR CONTRIBUTION

ACKNOWLEDGEMENTS

FUNDING

REFERENCES

1   Heinrich, R., Neel, B. G. and Rapoport, T. A. (2002) Mathematical models of protein kinase signal transduction. Mol. Cell **9**, 957–970

2   Hornberg, J. J., Bruggeman, F. J., Binder, B., Geest, C. R., de Vaate, A. J., Lankelma, J., Heinrich, R. and Westerhoff, H. V. (2005) Principles behind the multifarious control of signal transduction. ERK phosphorylation and kinase/phosphatase control. FEBS J. **272**, 244–258

3   Tonks, N. K. (2006) Protein tyrosine phosphatases: from genes, to function, to disease. Nat. Rev. Mol. Cell Biol. **7**, 833–846

4   Wishart, M. J. and Dixon, J. E. (1998) Gathering STYX: phosphatase-like form predicts functions for unique protein-interaction domains. Trends Biochem. Sci. **23**, 301–306

5   Tonks, N. K. (2009) Pseudophosphatases: grab and hold on. Cell **139**, 464–465

6   Alessi, D. R., Sakamoto, K. and Bayascas, J. R. (2006) LKB1-dependent signaling pathways. Annu. Rev. Biochem. **75**, 137–163

7   Wishart, M. J., Denu, J. M., Williams, J. A. and Dixon, J. E. (1995) A single mutation converts a novel phosphotyrosine binding domain into a dual-specificity phosphatase. J. Biol. Chem. **270**, 26782–26785

8   Blanchetot, C., Chagnon, M., Dube, N., Halle, M. and Tremblay, M. L. (2005) Substrate-trapping techniques in the identification of cellular PTP targets. Methods **35**, 44–53

9   Flint, A. J., Tiganis, T., Barford, D. and Tonks, N. K. (1997) Development of "substrate-trapping" mutants to identify physiological substrates of protein tyrosine phosphatases. Proc. Natl. Acad. Sci. U.S.A. **94**, 1680–1685

10 Wishart, M. J. and Dixon, J. E. (2002) The archetype STYX/dead-phosphatase complexes with a spermatid mRNA-binding protein and is essential for normal sperm production. Proc. Natl. Acad. Sci. U.S.A. **99**, 2112–2117

11 Bonifacio, E., Lampasona, V. and Bingley, P. J. (1998) IA-2 (islet cell antigen 512) is the primary target of humoral autoimmunity against type 1 diabetes-associated tyrosine phosphatase autoantigens. J. Immunol. **161**, 2648–2654

12 Kim, S. J., Jeong, D. G., Jeong, S. K., Yoon, T. S. and Ryu, S. E. (2007) Crystal structure of the major diabetes autoantigen insulinoma-associated protein 2 reveals distinctive immune epitopes. Diabetes **56**, 41–48

13 Torii, S. (2009) Expression and function of IA-2 family proteins, unique neuroendocrine-specific protein-tyrosine phosphatases. Endocr. J. **56**, 639–648

14 Drake, P. G., Peters, G. H., Andersen, H. S., Hendriks, W. and Moller, N. P. (2003) A novel strategy for the development of selective active-site inhibitors of the protein tyrosine phosphatase-like proteins islet-cell antigen 512 (IA-2) and phogrin (IA-2β). Biochem. J. **373**, 393–401

15 Hu, Y. F., Zhang, H. L., Cai, T., Harashima, S. and Notkins, A. L. (2005) The IA-2 interactome. Diabetologia **48**, 2576–2581

16 Nam, H. J., Poy, F., Krueger, N. X., Saito, H. and Frederick, C. A. (1999) Crystal structure of the tandem phosphatase domains of RPTP LAR. Cell **97**, 449–457

17 Wilks, A. F. (2008) The JAK kinases: not just another kinase drug discovery target. Semin. Cell Dev. Biol. **19**, 319–328

18 Persson, C., Sjoblom, T., Groen, A., Kappert, K., Engstrom, U., Hellman, U., Heldin, C. H., den Hertog, J. and Ostman, A. (2004) Preferential oxidation of the second phosphatase domain of receptor-like PTP-alpha revealed by an antibody against oxidized protein tyrosine phosphatases. Proc. Natl. Acad. Sci. U.S.A. **101**, 1886–1891

19 Cheng, K. C., Klancer, R., Singson, A. and Seydoux, G. (2009) Regulation of MBK-2/DYRK by CDK-1 and the pseudophosphatases EGG-4 and EGG-5 during the oocyte-to-embryo transition. Cell **139**, 560–572

20 Begley, M. J. and Dixon, J. E. (2005) The structure and regulation of myotubularin phosphatases. Curr. Opin. Struct. Biol. **15**, 614–620

21 Robinson, F. L. and Dixon, J. E. (2006) Myotubularin phosphatases: policing 3-phosphoinositides. Trends Cell Biol. **16**, 403–412

22 Robinson, F. L. and Dixon, J. E. (2005) The phosphoinositide-3-phosphatase MTMR2 associates with MTMR13, a membrane-associated pseudophosphatase also mutated in type 4B Charcot-Marie-Tooth disease. J. Biol. Chem. **280**, 31699–31707

23 Azzedine, H., Bolino, A., Taieb, T., Birouk, N., Di Duca, M., Bouhouche, A., Benamou, S., Mrabet, A., Hammadouche, T., Chkili, T. et al. (2003) Mutations in *MTMR13*, a new pseudophosphatase homologue of MTMR2 and Sbf1, in two families with an autosomal recessive demyelinating form of Charcot-Marie-Tooth disease associated with early-onset glaucoma. Am. J. Hum. Genet. **72**, 1141–1153

24 Siligan, C., Ban, J., Bachmaier, R., Spahn, L., Kreppel, M., Schaefer, K. L., Poremba, C., Aryee, D. N. and Kovar, H. (2005) EWS-FLI1 target genes recovered from Ewing's sarcoma chromatin. Oncogene **24**, 2512–2524

25 Owens, D. M. and Keyse, S. M. (2007) Differential regulation of MAP kinase signalling by dual-specificity protein phosphatases. Oncogene **26**, 3203–3213

26 Irvine, K., Stirling, R., Hume, D. and Kennedy, D. (2004) Rasputin, more promiscuous than ever: a review of G3BP. Int. J. Dev. Biol. **48**, 1065–1077

27 Myers, M. P., Stolarov, J. P., Eng, C., Li, J., Wang, S. I., Wigler, M. H., Parsons, R. and Tonks, N. K. (1997) P-TEN, the tumor suppressor from human chromosome 10q23, is a dual-specificity phosphatase. Proc. Natl. Acad. Sci. U.S.A. **94**, 9052–9057

28 Parker, F., Maurier, F., Delumeau, I., Duchesne, M., Faucher, D., Debussche, L., Dugue, A., Schweighoffer, F. and Tocque, B. (1996) A Ras-GTPase-activating protein SH3-domain-binding protein. Mol. Cell. Biol. **16**, 2561–2569

29 Tourriere, H., Chebli, K., Zekri, L., Courselaud, B., Blanchard, J. M., Bertrand, E. and Tazi, J. (2003) The RasGAP-associated endoribonuclease G3BP assembles stress granules. J. Cell Biol. **160**, 823–831

30 Pazman, C., Mayes, C. A., Fanto, M., Haynes, S. R. and Mlodzik, M. (2000) Rasputin, the *Drosophila* homologue of the RasGAP SH3 binding protein, functions in Ras- and Rho-mediated signaling. Development **127**, 1715–1725

31 Gallouzi, I. E., Parker, F., Chebli, K., Maurier, F., Labourier, E., Barlat, I., Capony, J. P., Tocque, B. and Tazi, J. (1998) A novel phosphorylation-dependent RNase activity of GAP-SH3 binding protein: a potential link between signal transduction and RNA stability. Mol. Cell. Biol. **18**, 3956–3965

32 Tourriere, H., Gallouzi, I. E., Chebli, K., Capony, J. P., Mouaikel, J., van der Geer, P. and Tazi, J. (2001) RasGAP-associated endoribonuclease G3Bp: selective RNA degradation and phosphorylation-dependent localization. Mol. Cell. Biol. **21**, 7747–7760

33 Barnes, C. J., Li, F., Mandal, M., Yang, Z., Sahin, A. A. and Kumar, R. (2002) Heregulin induces expression, ATPase activity, and nuclear localization of G3BP, a Ras signaling component, in human breast tumors. Cancer Res. **62**, 1251–1255

34 Guitard, E., Parker, F., Millon, R., Abecassis, J. and Tocque, B. (2001) G3BP is overexpressed in human tumors and promotes S phase entry. Cancer Lett. **162**, 213–221

35 Kedersha, N., Stoecklin, G., Ayodele, M., Yacono, P., Lykke-Andersen, J., Fritzler, M. J., Scheuner, D., Kaufman, R. J., Golan, D. E. and Anderson, P. (2005) Stress granules and processing bodies are dynamically linked sites of mRNP remodeling. J. Cell. Biol. **169**, 871–884

36 Tourriere, H., Chebli, K. and Tazi, J. (2002) mRNA degradation machines in eukaryotic cells. Biochimie **84**, 821–837

37 Kedersha, N. L., Gupta, M., Li, W., Miller, I. and Anderson, P. (1999) RNA-binding proteins TIA-1 and TIAR link the phosphorylation of eIF-2α to the assembly of mammalian stress granules. J. Cell. Biol. **147**, 1431–1442

38 Huang, Y., Wernyj, R. P., Norton, D. D., Precht, P., Seminario, M. C. and Wange, R. L. (2005) Modulation of specific protein expression levels by PTEN: identification of AKAP121, DHFR, G3BP, Rap1, and RCC1 as potential targets of PTEN. Oncogene **24**, 3819–3829

39 Kim, M. M., Wiederschain, D., Kennedy, D., Hansen, E. and Yuan, Z. M. (2007) Modulation of p53 and MDM2 activity by novel interaction with Ras-GAP binding proteins (G3BP). Oncogene **26**, 4209–4215

40 Arimoto, K., Fukuda, H., Imajoh-Ohmi, S., Saito, H. and Takekawa, M. (2008) Formation of stress granules inhibits apoptosis by suppressing stress-responsive MAPK pathways. Nat. Cell Biol. **10**, 1324–1332